SELF-CONSISTENT SIMULATION OF PLASMA INTERACTIONS WITH SECONDARY-EMITTING INSULATORS

S. T. Brandon, R. L. Rusk, T. P. Armstrong, and J. Enoch
University of Kansas
Lawrence, Kansas 66045

A cylindrical particle-in-cell (PIC) plasma simulation code applicable to plasma densities encountered in low earth orbit (LEO) is nearing completion. The simulated geometries include that of a plain disk and a disk surrounded by a dielectric. Both configurations are mounted upon a ground plate in contact with a plasma environment. Techniques allowing simulation of dielectric charging using PIC time scales are discussed. Current versus voltage characteristic curves are calculated and the results are compared to experimental data.

INTRODUCTION

The plasma densities present in LEO (10^4 - 10^6 /cm^3) may cause the collection of large plasma coupling currents for spacecraft operating at high voltages. In particular, large high-voltage solar cell arrays exposed to the LEO environment could collect enough parasitic current from the ambient plasma to degrade their performance. Additionally, exposed dielectric material can develop large differential potentials. Punctures in insulators over conductors have been seen to collect currents much larger than would be expected based on the area of the exposed conductor (ref. 1).

In this paper, a status report of the results of a continuing effort to develop a self-consistent numerical simulation to explore more thoroughly the interactions of an ambient plasma with a conducting disk, which may be partially covered with a dielectric material, is presented. The disk surrounded by dielectric material represents a hole in an insulator covering a conductor. The background plasma parameters are chosen to resemble conditions of LEO. Since all particle trajectories are known, any process which can be modeled statistically for a single plasma particle can be included by the simulation code. Plasma interactions currently considered include the effects of charge collection on the dielectric and secondary electron emission. The simulation region includes a ground plate on which the disk or disk and dielectric are mounted. The resulting configuration closely matches the experiments (ref. 2).

This combination of geometry and plasma parameters incorporates the basic physics of the interactions which would be present between a high voltage solar cell array and the plasma environment. Yet, unlike the solar array, the geometry is simple enough to be handled by a particle-pushing code. Although a ratio of ion to electron mass of 1:1 is commonly used, mass ratios of 100:1 or higher can be handled. This allows the simulation of

negative voltages present upon the central conductor. Thus, information gained from an analysis of the disk and dielectric configuration will be directly applicable to the design of large-scale, high-voltage solar cell arrays meant to be placed in low earth orbit.

REVIEW OF THE SIMULATION MODEL

The plasma simulation code is a further development of the 2-1/2 dimensional program described previously (refs. 3 to 6). The cylindrical simulation region is divided into a numerical grid which is used to calculate the potentials and fields of the problem. The calculational grid is shown in figure 1. Each cell represents a ring of space due to rotational symmetry about the Z-axis (boundary region 1). Boundary regions 2 and 3 represent the outer boundaries of the calculation. The outer boundaries are assumed to be removed far enough from the conducting disk so that potentials imposed upon the disk do not affect the boundaries. Thus, the plasma is maxwellian at the outer boundaries and the potential is set to zero. Particles are added to the simulation along boundaries 3 and 4 according to the value of the random thermal current. Particles are lost to the simulation whenever their orbits cross one of these two boundaries. Boundary region 4 represents the ground plate. The potential on boundary region 4 is set to zero and all particles intersecting this boundary are absorbed. The surface of the dielectric covering part of the conductor is represented by boundary region 5 (may have zero length). All particles striking boundary region 5 are absorbed. Electrons striking the dielectric may emit secondaries with their number distribution given by fits to experimental data presented by Haffner (ref. 7). The potential on the surface of the dielectric is determined by the following equation:

$$\Phi(\delta) = \frac{\delta}{\epsilon}\left[4\pi\sigma + \frac{\epsilon}{\delta}\Phi(0)\right] + \epsilon\Phi(\Delta z) \tag{1}$$

where δ is the thickness of the dielectric, ϵ is the dielectric constant, σ is the charge per unit area, and $\Phi(0)$ is the potential of the conducting disk. This is just an infinite capacitor approximation which may not be valid near the edges of the dielectric surface. Boundary region 6 represents the exposed portion of the conducting disk which can be set at a desired potential with respect to the potential of the plasma exterior to the simulation region (zero). Particles which enter boundary region 6 are absorbed and form the current drawn by the conductor from the plasma.

The simulation code is based upon standard PIC simulation techniques whenever possible. An overview of the program is shown in figure 2. The initial particles are randomly added to the simulated space with velocities chosen from a maxwellian distribution. This represents a nonequilibrium situation unless a potential of zero is specified on the conductor. The equations of motion are integrated using a second-order leap-frog method. To avoid the singularity present in the cylindrical equations of motion as r approaches zero, cartesian coordinates are used to compute particle movement. The coordinates are converted back into the cylindrical form when

the move is completed. The particle mover advances particles through the simulation in increments of the time step value. The time step value is set such that the fastest particles move less than 1 grid cell per time step (about 10^{-9} sec). Particles are added at the outer boundaries from the surrounding undisturbed plasma (assumed to have a maxwellian velocity distribution, usually of 10,000 deg K, about 1 eV). All particles present which have entered any of the sink regions are discarded. The remaining particle charges are spread over the grid using volume weighting over the nearest grid cells. Successive over-relaxation with odd-even stepping is used to solve Poisson's equation - yielding a self-consistent calculation of the electrostatic potential. The electric field can then be calculated by differentiating the potential.

The total number of time steps simulated may range from about 4000 time steps for the plain disk configuration to 20,000 time steps for the disk and dielectric configuration. The average age of particles within the simulations for the 20x20 grid is about 100 time steps. This implies a complete cycling of particles in the simulation space occurring about 200 times for a 20,000 time step simulation. Hence, plasma parameters such as temperature and density are determined by the additions of particles on the outside boundaries, not by the initial particle distribution. It is important to ensure that the program can maintain a constant density and temperature for a free plasma over many time steps. Simulation of a free plasma is accomplished by setting the radius of the conductor to zero (extending boundary region 4 over the entire lower boundary) and reflecting any particles which cross boundary region 4. The potential on boundary region 4 is set to zero. A plot of the total number of particles present in the simulation region versus time step number is shown in figure 3. The initial number of particles (2000 per species) remains constant within statistical fluctuations for the entire 8000 time steps computed using a 20x20 calculational grid size. The average kinetic energy per particle remains constant as shown in figure 4. Thus the simulation code has been shown to be able to simulate a free plasma for a large number of time steps without undergoing any nonphysical instabilities.

This simulation program is applicable when the plasma Debye length is of about the same order of magnitude as the disk radius. Large plasma densities would cause large fluctuations in the collected current, since this calculation makes use of a small number of particles. The PIC assumptions made also imply that the Debye length is larger than one grid cell. With these restrictions and probe sizes ranging from 1.75 cm to 10.0 cm in radius and with electron and ion temperatures of about 1 eV, plasma densities are then about 10,000 particles per cubic centimeter. This corresponds to environments encountered in the upper ionosphere or low earth orbit. The Debye length under these conditions is about 5 cm.

PLAIN DISK CALCULATIONS

Approach to Equilibrium

The plain disk or electrostatic probe configuration is the simplest configuration simulated. The rapid approach to equilibrium is demonstrated in figure 5. Voltage versus current density curves drawn by the disk are shown for simulation runs of various durations. The value for the current can be

seen to achieve an equilibrium state after 2000 time steps of the simulation have been completed. Since only two or three thousand time steps need be taken, a large number of runs may be made for the disk only case using a relatively small amount of computer time (1 minute on the CRAY I, and 36 minutes for the VAX 11/750 with a 4000 time step run). Thus the plain disk simulations can be used to explore a wide range of plasma parameters and establish areas of applicability for the more complex disk and dielectric simulations.

Comparison with Experiment

The comparison with experiment (ref. 2) is displayed by figure 6. The experimental current-voltage curve is shown for a plasma density of 20,000 particles per cubic centimeter and a disk radius of 1.75 cm. The only modification to the experimental curve has been the correction of -8 volts so that voltages in both the simulation and the experiment will be referenced to the plasma potential, and not to the vacuum chamber wall. In spite of experimental uncertainties in the plasma parameters and statistical errors present in the simulations, the experiment and calculated values of the collected current versus voltage are in good agreement.

The calculated curve was constructed as a hybrid of three separate series of computer runs. The voltage points between 20 and 200 volts were obtained using a 10x10 grid simulation running for 3200 time steps on a VAX 11/750 computer. The lower voltage points were also calculated with a 10x10 grid simulation, but 16,000 time steps were necessary to reduce the statistical fluctuations. The higher voltages were simulated with a 20x20 grid utilizing the same spacial resolution as the other 10x10 grid calculations. Both the lower and higher voltage points were computed on a CRAY I machine.

The negative voltage experimental curve can also be compared to the positive voltage simulation results. The current collected by the positive voltage simulations is scaled by the square root of the mass ratio (for a nitrogen plasma the scale factor is 160) to produce the expected results of a negative voltage run. This comparison is shown in figure 7. The agreement between simulation and experiment is not as good as for the positive voltages. The simulation collects about 1/2 of the current of the experiment throughout the voltage range. This is within the experimental uncertainties and simulation statistical error. However, unlike the positive voltage case, the mean values of the collected current do not agree. This indicates that current scaling by the square root of the mass ratio for negative voltages (large ion to electron mass ratios) is only approximate.

Simulation of Large Mass Ratios

For the disk only configuration, the current collected by the positive voltage calculation can be scaled to the expected current that would be seen in a negative voltage simulation. For the disk and dielectric configuration the current scaling to negative voltages is inappropriate due to the presence of a dielectric surface which will charge differently in the two voltage ranges. The charging of the dielectric will also depend upon the ratio between the ion and electron mass. With the normal 1:1 mass ratio, the dielectric surface, when exposed to the plasma, will not charge, in spite of

290

the fact that the increased mobility of the electrons should charge the surface of the dielectric negatively. In order to be able to realistically simulate dielectric charging effects and negative voltages for the disk and dielectric configuration, it is necessary to relax the PIC requirement of 1:1 mass ratios.

The disk only configuration provides an excellent test of the methods developed to handle larger mass ratios. This configuration is simple and gives simulation results with a minimum of CPU time. The expected collected current for each mass ratio can be found by simply scaling the positive voltage result to the negative voltage simulation value. The diagnostics furnished are excellent.

The usual way to handle larger mass ratios is to simply give the ions a larger mass value. This method has several disadvantages. Since the simulation procedure is not affected, it takes the same CPU time per time step to simulate larger mass ratios as it would to simulate a 1:1 mass ratio. The distance each ion would move per time step decreases with the increasing value of the mass ratio. Thus, for reasonable mass ratios (hydrogen plasma, 1836:1), the simulation would have to be run many times longer (at the same relative speed) to come to equilibrium. Also the ion motion per time step might become so small as to be dominated by roundoff error. This generally limits PIC simulations to various small values of the mass ratio. From these results, speculations are made as to the effect of realistic mass ratios.

Another method to simulate large mass ratios can be developed. The relatively slow movement of the ions per time step indicates that it is a wasted effort to move them every time step. Instead, ions can be moved once every n time steps. In this case n is chosen to be large enough so the ions move about the same average distances every n time steps as they would in a simulation run with a mass ratio of 1:1 for each time step. Thus ion and electron particle movement are restored to a relative parity at the expense of the additional assumption that the electric fields remain constant (at least in the average) for n time steps. The constant electric field assumption is clearly invalid at the beginning of a run. However, once a simulation reaches an equilibrium state, the assumption of a constant electric field should be justified. Once again it is postulated that if the simulation is run until an equilibrium state is reached, details about the approach to the equilibrium are lost - implying the equilibrium state is unique.

The remaining problem is to determine n for a given mass ratio in such a manner that the least amount of extra computing is required. The particle's energy should remain constant as the mass ratio is varied. Therefore, the ion velocity is proportional to the square root of the inverse of its mass ratio. The time period over which the ions are moved then is just proportional to the square root of their mass ratio. The simulated mass ratio should be chosen such that its square root is an integer.

The above algorithm can be implemented with the PIC code by the following simple procedure. The form of the equations of motion describing the R coordinate which are solved by the particle mover are:

$$m(V_{r,new} - V_{r,old}) = \Delta t \left(\frac{l^2}{mr^3} + qE_r \right) \tag{2}$$

$$r_{new} = r_{old} + \Delta t V_{r,new} \tag{3}$$

Since the energies of particles with differing mass ratios are constant at each point along the trajectory, the angular momentum term, l^2/mr^3, remains constant under variations of the ion mass ratio. The combined effects of substituting $m'=n^2m$ and $\Delta t'=n\Delta t$ just cancel in the equations of motion. A similar behavior is found for the equations of motion describing the Z coordinate. Thus, mass ratios of n^2:1 can be simulated simply by moving the ions only once every n time steps.

Results obtained by using the direct and indirect methods to simulate large mass ratios have no effect on the current collected by the disk for positive voltages. The collected current is dominated by electrons; any difference in the ion mass is not seen. The best test of the larger mass ratio simulation methods is the simulation of negative voltages on the conductor. In this case the ions dominate the current and the electrons are excluded from the conductor. Results of simulations using several different mass ratios by both methods are shown in figure 8. The expected current which would be collected by the conductor decreases with increasing mass ratios. The general shape of the current-voltage curve remains intact for both approximations down to mass ratios of 4:1. For mass ratios of 100:1, the straightforward method of computing mass ratio effects using a larger mass value begins to collect more current than the simulations which move the ions once per every 10 time steps. When a mass ratio of 1849:1 is attempted, by moving the ions once per 43 time steps, the current-voltage curve begins to bend over. This could be caused by a lack of statistics (30,000 time steps result in only 700 ion movements) or possibly the assumption of constant electric fields over the 100 time step interval is beginning to break down.

THE DISK AND DIELECTRIC CONFIGURATION

The Approach to Equilibrium

The final equilibrium situation of the disk and dielectric is much harder to identify than that of the plain disk. The capacitance inherent in the dielectric causes the response time for charging to be large compared with the plasma frequency. Typically the dielectric may slowly charge or discharge during the simulation run, imitating an equilibrium situation in the steadiness of the current values obtained. It is important to take a detailed look at the available history information to determine whether a run reached an equilibrium state. For quick inspections, the value of the total charge collected by the dielectric is usually the most sensitive indicator of equilibrium. In practice it has been difficult to run current-voltage points long enough to arrive at an equilibrium value. Techniques have been developed to make the calculation come into an equilibrium state in a reasonable number of time steps.

One way to reach equilibrium is simply to run the simulation long enough (many plasma periods) until the equilibrium-state is found. This method was tried for the 10x10 grid with 500 particles per species. A time history plot of the total charge on the dielectric obtained from a 20,000 time step run made at 10 volts is shown in figure 9. Beginning with an uncharged dielectric, charge accumulates rapidly for about the first 15,000 time steps. Due to the uniformly decreasing value of the slope of the curve, it is difficult to determine the onset of the equilibrium situation.

The first method implemented to speed the approach to equilibrium is based upon the observation that the dielectric generally charges until its potential decreases to zero (the voltage is lower than the first crossover point for secondary emission). If most of the charge needed to reach zero potential is added during the initialization, less time will be spent collecting charge during the run. Effects of loading the dielectric with different amounts of charge are also shown in figure 9. All runs come to the same equilibrium, which suggests that the equilibrium is unique. This method of decreasing the time to reach equilibrium proves to be ineffective at higher voltages. The dielectric must collect more particles to charge to an equilibrium value than are added at the boundaries during the 20,000 time steps of the calculation.

The relationship which causes the simulation to approach equilibrium slowly is contained in the boundary condition imposed upon the dielectric (equation 1). The leading factor of the thickness of the dielectric over the dielectric constant is usually small (in the previous runs we have used a value of 1/28 as opposed to the experimental value of 1/280 in order to keep this ratio large enough to be somewhat manageable). The small value of δ/ε means that a large amount of simulation time will be used to accumulate this charge. The second method implemented to speed up the approach to equilibrium was the introduction of artificially high values for δ/ε. The physical effects of increasing δ/ε can be thought of in one of several ways:

1. a decrease in the capacitance associated with the dielectric
2. an introduction of an artificial dielectric thickness
3. artificially increasing the charge collected by the dielectric

The result of a 10 volt run with a 10x10 grid of 500 particles per species is shown in figure 10. The time history graph of the total charge collected by the dielectric shows that equilibrium is reached after about 500 time steps for a value of $(\delta/\varepsilon)^*$ set to 1.

The artificial value of $(\delta/\varepsilon)^*$ must be chosen with care. If the value is too small, equilibrium still will not be reached. If the value is too large, the potential on the dielectric will vary dramatically with the collection of only small numbers of particles (one). Assuming a constant charging rate proportional to the thermal current leads to the following expression:

$$\left(\frac{\delta}{\varepsilon}\right)^* = C \frac{V}{(\Delta t)(n)(T)^{1/2}} \tag{4}$$

where V is the voltage on the conductor, Δt is the time step value, n is the electron density, T is the electron temperature, and C is the proportionality

constant. Substituting values of the other variables for the above 10 volt run determines C (.4824).

The artificial value of $(\delta/\varepsilon)^*$ computed with the above equation assumes the number of particles present is large enough so that non physical effects associated with the granularity of charge collected on the dielectric do not occur. In practice, the value of $(\delta/\varepsilon)^*$ must be kept small enough that the change in the potential on the dielectric surface per particle impact is only a small fraction of the potential applied to the conductor (1%). The upper limit of the value of $(\delta/\varepsilon)^*$ is then given as follows:

$$\left(\frac{\delta}{\varepsilon}\right)^* = \frac{0.0075(dr)V}{q} \qquad (5)$$

where dr is the length of a grid cell and q is the charge per macroparticle.

Comparison with Experiment

The resulting current-voltage curves for the disk and dielectric configuration are shown in figure 11 for a disk radius of 1.75 cm and a dielectric radius of 8.75 cm. The simulation with a mass ratio of 1:1 collects the same amount of current as the plain disk (the size of the exposed conductor is the same) for low voltages. As the voltage on the conductor is raised, a point is reached where the current collected by the disk surrounded with dielectric material increases compared to that of the plain disk. This increase in collected current is due to the presence of the dielectric and occurs when the dielectric begins to come to an equilibrium with positive potentials near the conducting disk. The dielectric will charge to positive values when the average number of secondaries released by the impacting primary electrons is greater than one. The point at which this occurs is determined by details of the secondary emission yield curve for the dielectric and by the energy spectrum of the primary particles. The calculated current-voltage characteristic curve shows a current enhancement beginning at a lower voltage than that found in the experiment.

Also shown in figure 11 are calculated current-voltage curves for mass ratios of 4:1 and 100:1. The larger mass ratios allow the surface to charge negatively for low voltages. The negative voltages present on the dielectric reduce the collection of electrons by the conductor for low voltages. As the voltage on the conductor is increased, the surface of the dielectric begins to become positive, as in the 1:1 mass ratio case. From this point on, the current remains almost unaffected by the ion mass ratio. These current-voltage curves show qualitatively correct behavior using the correct boundary conditions.

Variations of the Secondary Electron Emission Yield Parameter

The effect of variations in σ_m, the maximum number of electrons scattered from the dielectric surface per incoming primary electron, upon the current voltage curves is shown in figure 12. The voltage of the onset of

the increase in collected current with reference to the plain disk decreases with increasing σ_m. The increase in σ_m lowers the energy of the first crossover for secondary emission. Also, the number of secondaries released for energies larger than the first crossover point increases. Both effects create more secondary emission at lower voltages than would normally be found. The sensitivity of the calculation to the secondary electron production might be sufficient to allow the measurement of the yield curve parameters for low voltages by fitting the response to experimental data.

A detailed examination of the potential present along the top of the dielectric during a simulation run which collected more current than that of the plain disk reveals what is happening. The initial condition shown in figure 13 for time step zero is a fully charged dielectric; the potential on the dielectric surface is zero. This would be realistic if the voltage on the conductor were increased slowly from a value low enough that the dielectric surface became fully charged. As the simulation proceeds, the potential upon the dielectric remains unstable, but positive for the first 6,000 time steps. After the equilibrium situation is reached, the potential remains constant to the termination of the run after 20,000 time steps. The equilibrium potential over the dielectric is uniformly positive and decreasing in value from the voltage on the exposed conductor to near zero at the outside edge of the dielectric. The potentials behave as if they have "snapped over" from their normal near zero level. This resembles the snapover phenomenon observed in experiments with solar cell arrays (ref. 2). The potential upon the cover slips for the array increased from values near zero below 100 volts to values about 50 volts less than that of the interconnects for voltages greater than about 200 volts.

CONCLUDING REMARKS

A cylindrical particle-in-cell plasma simulation code applicable to plasma densities encountered in low earth orbit is nearing completion. Results of the calculation of plasma coupling current for the plain disk are in agreement with experiment for positive voltages. Any deficiencies in the simulation of the disk and dielectric configuration are due solely to the interactions of the dielectric. Techniques have been developed which allow dielectric charging to occur at PIC time scales. The current-voltage characteristic curves are in qualitative agreement with experiment, indicating that for these voltage ranges charge sticking and secondary emission probably adequately describe the dielectric interactions with the ambient plasma. The amount of secondary emission from the dielectric at low voltages during the simulations needs to be reduced to match the experimental current-voltage characteristic curve. Calculations using large ion to electron mass ratios are made possible by restricting both the grid size and particle number and simulating the mass ratio effects by moving the ions once for every n time steps. The square root of the desired ion to electron mass ratio determines the value of n. Further computational effort is required to extend the range of the disk and dielectric simulations to higher voltages and larger mass ratios.

REFERENCES

1. Domitz, Stanley and Norman T. Grier, "The interaction of spacecraft high voltage power systems with the space plasma environment.", NASA TM X-71554, 1974.

2. Stevens, N. J., F. D. Berkopec, C. K. Purvis, N. Grier, and J. Staskus, "Investigation of high voltage spacecraft interactions with plasma environments.", AIAA/DGLR 13th International Electric Propulsion Conference Paper 78-672, 1978

3. Nonnast, J. H., "Numerical simulation of a disk-shaped electron accelerating electrostatic probe.", J. Appl. Phys. 54-2, 1983, pp. 621-631.

4. Chaky, R. C., J. H. Nonnast, and J. Enoch, "Numerical simulation of sheath structure and current-voltage characteristics of a conductor-dielectric in a plasma.", J. Appl. Phys. 52-12, 1981, pp. 7092-7098.

5. Nonnast, J. H., R. C. Chaky, T. P. Armstrong, J. Enoch, and G. G. Wiseman, "Numerical simulation of plasma-insulator interactions in space, Part I: The self-consistent calculation.", Spacecraft Charging Technology - 1980, NASA CP-2182, 1981.

6. Chaky, R. C., J. H. Nonnast, T. P. Armstrong, J. Enoch, and G. C. Wiseman, "Numerical simulation of plasma-insulator interactions in space, Part II: Dielectric effects.", Spacecraft Charging Technology - 1980, NASA CP-2182, 1981.

7. Haffner, J. W., "Secondary electron effects on spacecraft charging.", Spacecraft Charging Technology Conference, NASA CP-2071, 1978.
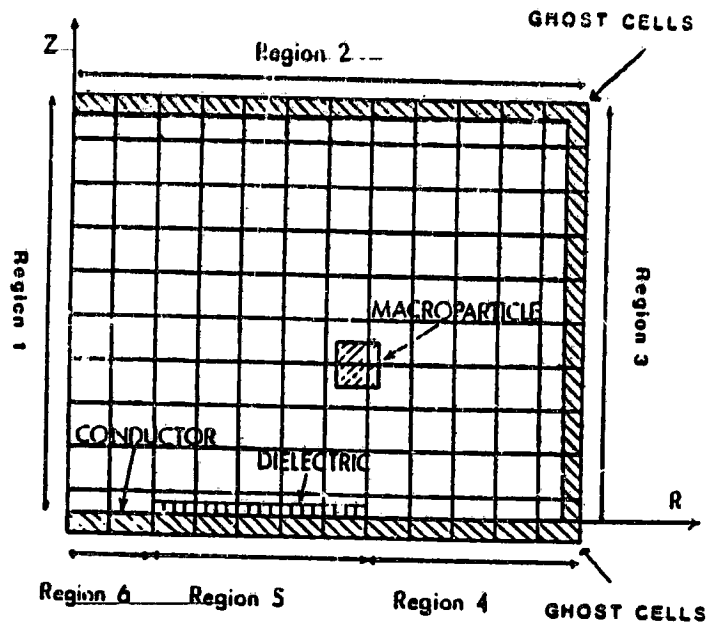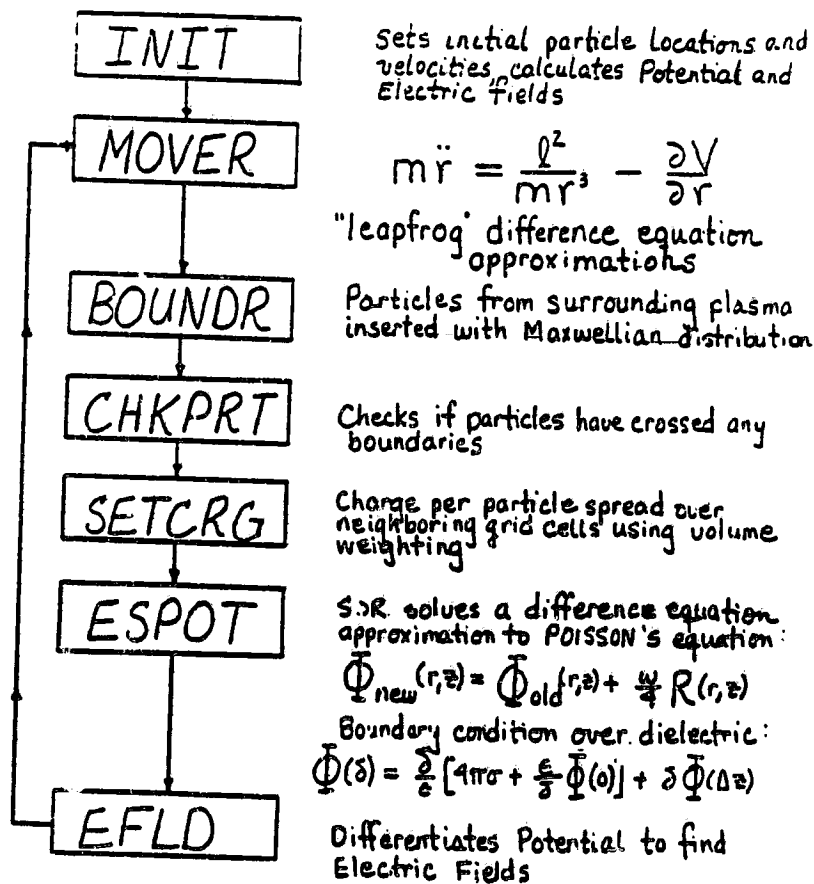
GHOST CELLS

Z

Region 2

Region 1

Region 3

MACROPARTICLE

CONDUCTOR

DIELECTRIC

R

Region 6   Region 5   Region 4   GHOST CELLS

Figure 1. – Simulation grid.

INIT — Sets initial particle locations and velocities, calculates Potential and Electric Fields

MOVER —
$$m\ddot{r} = \frac{\ell^2}{mr^3} - \frac{\partial V}{\partial r}$$
"leapfrog" difference equation approximations

BOUNDR — Particles from surrounding plasma inserted with Maxwellian distribution

CHKPRT — Checks if particles have crossed any boundaries

SETCRG — Charge per particle spread over neighboring grid cells using volume weighting

ESPOT — SOR solves a difference equation approximation to POISSON's equation:
$$\bar{\Phi}_{new}(r,z) = \bar{\Phi}_{old}(r,z) + \frac{\omega}{4} R(r,z)$$
Boundary condition over dielectric:
$$\bar{\Phi}(\delta) = \frac{2}{\epsilon}\left[4\pi\sigma + \frac{\epsilon}{\delta}\bar{\Phi}(0)\right] + \delta\bar{\Phi}(\Delta z)$$

EFLD — Differentiates Potential to find Electric Fields

Figure 2. – Overview of simulation code.
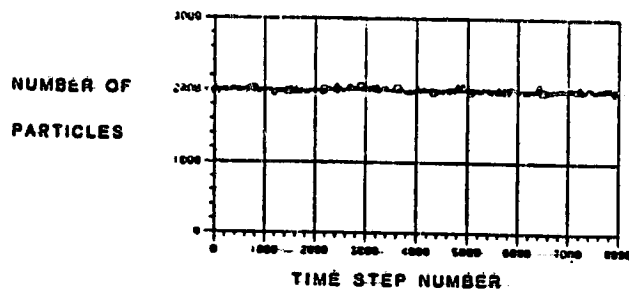
Figure 3. – Simulation of a free plasma – number of particles.
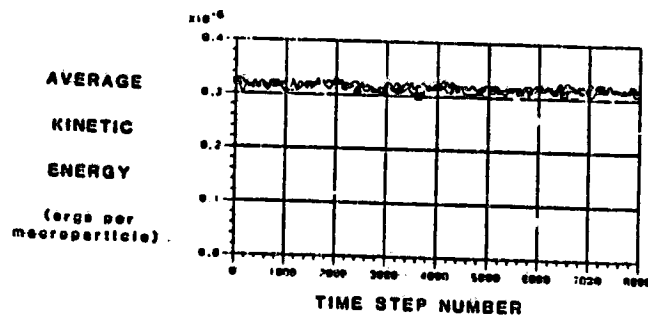
Figure 4. – Simulation of a free plasma – average kinetic energy.
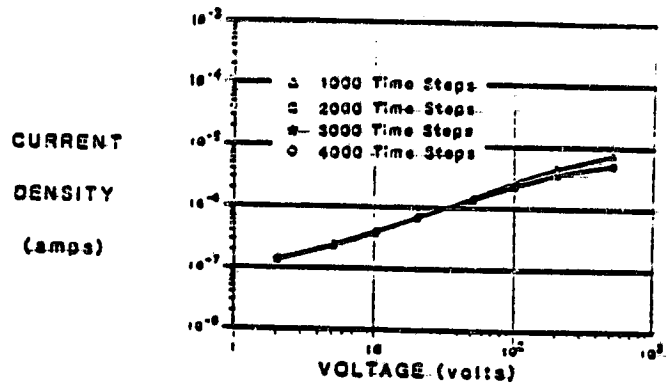
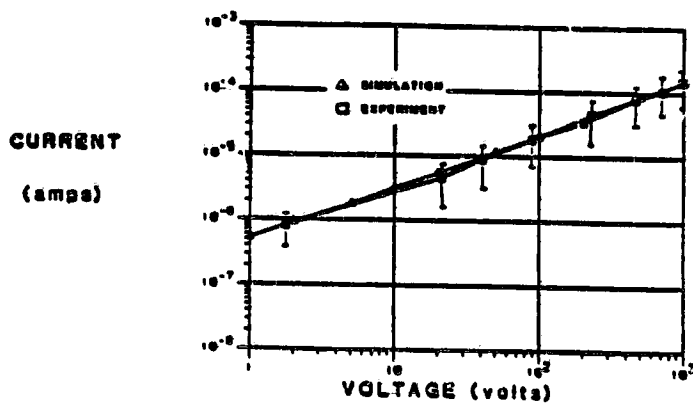Figure 5. – Approach to equilibrium – plain disk.

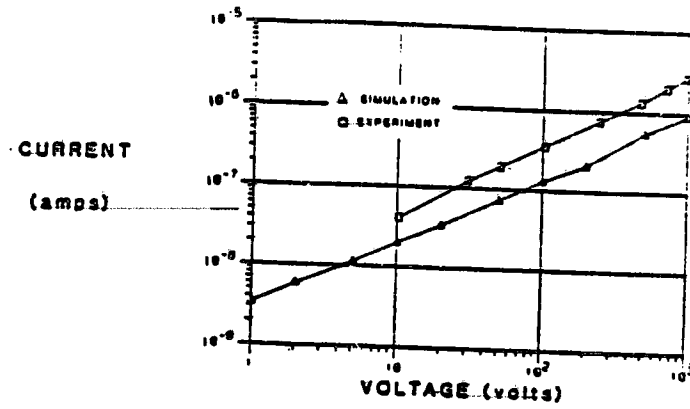Figure 6. – Comparison with experiment – positive voltage.

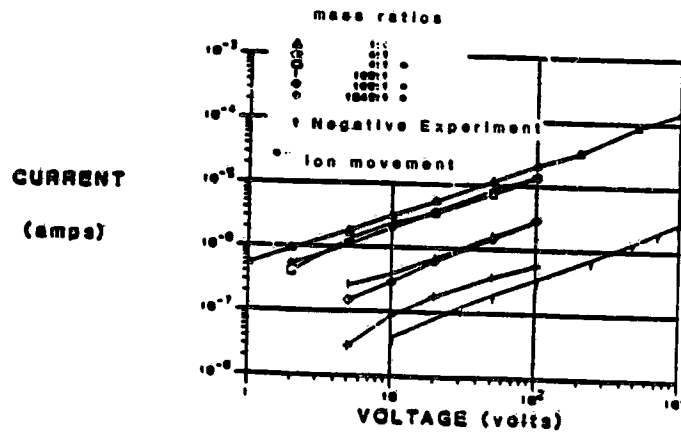Figure 7. – Comparison with experiment – negative voltage.
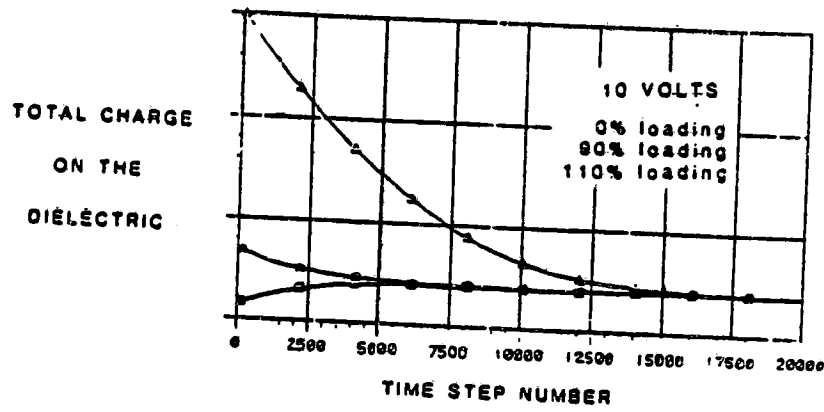

Figure 8.- Large mass ratio calculations.

TOTAL CHARGE

ON THE

DIELECTRIC

10 VOLTS

0% loading
90% loading
110% loading

TIME STEP NUMBER

Figure 9. – Approach to equilibrium – effects of loading dielectric with different amounts of charge.

TOTAL CHARGE

ON THE

DIELECTRIC

TIME STEP NUMBER
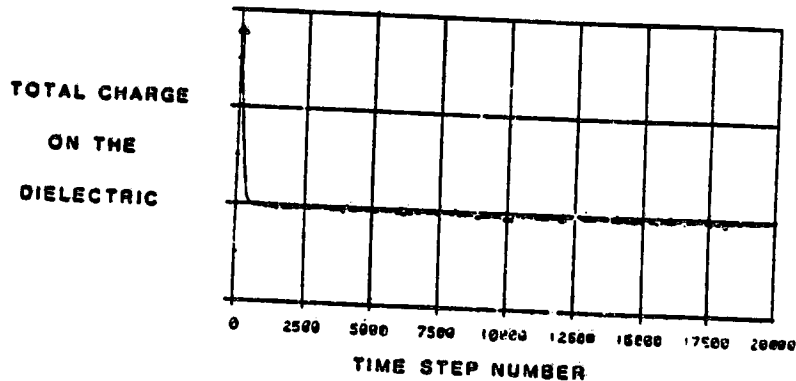
Figure 10. – Approach to equilibrium – effects of increasing δ/ϵ.

301
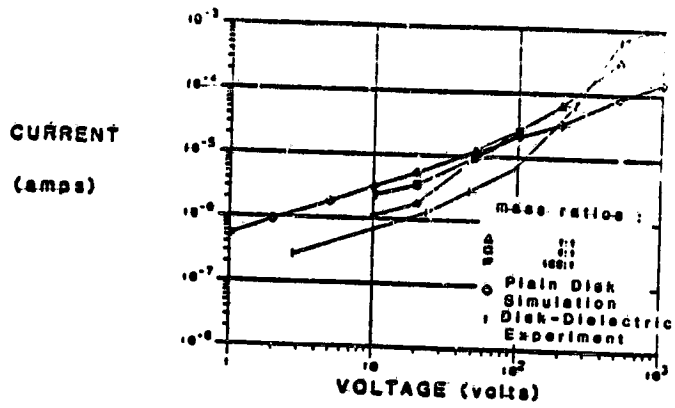
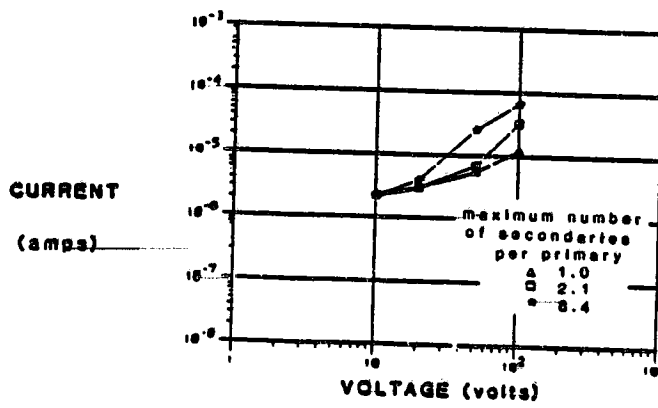Figure 11. – Disk and dielectric results.
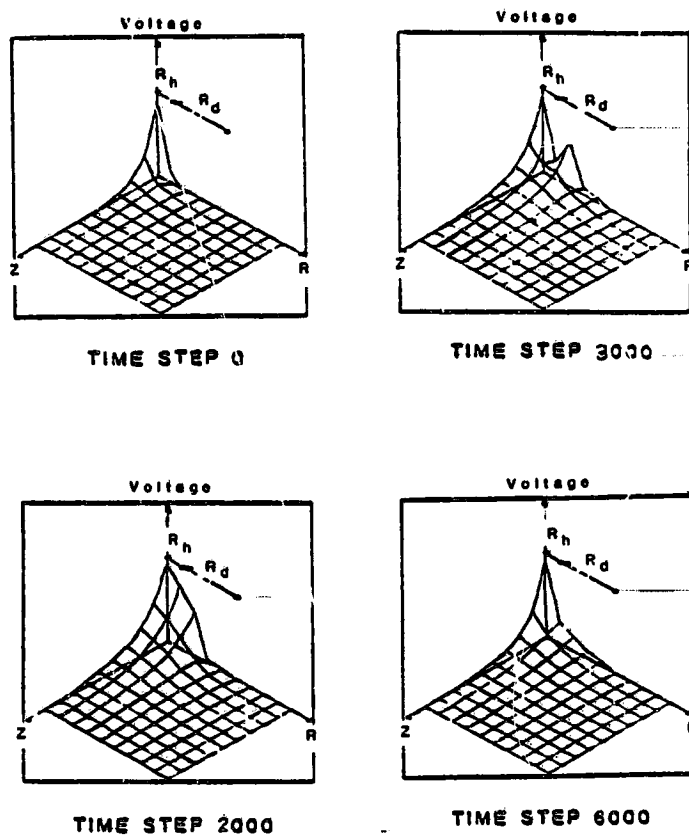

Figure 12. – Variations in secondary emission yields.

Figure 13. – Snapover effect (potential snapshots).